

Fig. 3 Temperature profiles at  $x = 1$  ft and 5 ft in transformed coordinate.

point boundary conditions at various distances along the wall. These solutions have been obtained by the usual method of assuming the boundary conditions at the wall and iterating until the boundary conditions at the outer edge are satisfied. In this way, locally similar solutions have been obtained to  $x = 5$  ft. However, even at this distance, the time and effort required to obtain the correct iterated boundary conditions is enormous and increases downstream from the leading edge since exceedingly accurate assumed boundary conditions are required there. To obtain these quantities the similar boundary-layer equations are solved near the leading edge where less accurate boundary conditions are required. Then one proceeds along the wall from the frozen toward the equilibrium regime extrapolating the boundary conditions and obtaining solutions further downstream.

To solve the complete partial differential equations of the nonequilibrium boundary layer an implicit finite difference procedure has been developed<sup>1</sup> which accounts for the "non-similar" terms not included in the forementioned system of equations. The flow along a wall with zero pressure gradient at an altitude of 100,000 ft ( $T_e = 392.4^\circ\text{R}$  and  $p_e = 23.4265$  psf) and a freestream velocity of 25,000 fps has been obtained with this numerical scheme. As these results employ the same assumptions about the gas as the similar solutions and approach the exact solution to the problem, the validity of using local similarity for this problem is evaluated. In Figs. 1 and 2 the temperature and atom mass fraction gradients at the wall are presented. These are the boundary conditions at the wall for the similar solution that must be assumed and iterated until the correct values are obtained. For this problem, the velocity profiles are obviously the Blasius result and do not change along the wall. The temperature and atom

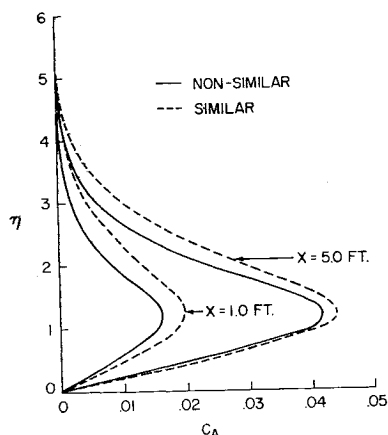


Fig. 4 Atom mass fraction profiles at  $x = 1$  ft and 5 ft in transformed coordinate.

mass fraction profiles at  $x = 1$  ft and 5 ft are presented in Figs. 3 and 4. These results indicate that the atom mass fraction profiles for the boundary layer with the local similarity assumption are in greatest error.

Even if one is willing to accept the accuracy of the similar solution, which is reasonable for this example, the difficulty of acquiring the results limits the usefulness of the procedure. The nonsimilar procedure gives more accurate results while requiring less time to obtain them.

#### Reference

- <sup>1</sup> Blottner, F. G., "Non-equilibrium laminar boundary layer flow of a binary gas," General Electric TIS R63SD17 (June 1963).

## Effect of Gravity on the Mobility of a Lunar Vehicle

GEORGE A. COSTELLO\*

University of Illinois, Urbana, Ill.

AND

DONALD L. DEWHIRST†

Chrysler Corporation, Detroit, Mich.

This paper presents a dimensional analysis for determining the effect of gravity on the tractive effort of a vehicle moving in a soil. The theory shows that the effect of lunar gravity may be simulated by changing controlled variables. Test results are presented for a six-wheel model operating in  $\frac{1}{4}$ -in. gravel. These results show that, for a vehicle traveling in a horizontal plane on a cohesionless soil, the percent slip, for a given ratio of drawbar pull to vehicle weight, is practically unaffected by changes in gravity.

#### Introduction

**S**IMULATION of lunar  $g$  can be accomplished by means of an accelerating platform, that is, by dropping the test apparatus at  $\frac{5}{8} g$ . However, this simulation must be necessarily of short duration.

In this paper, the effects of gravity are determined by employing dimensional analysis and test results. Dimensionless parameters are introduced and the effect of gravity is determined by varying these parameters.

#### Analysis

The variables that are assumed to be pertinent to the problem under consideration are listed below. The dimensions are given in terms of mass  $M$ , length  $L$ , and time  $T$ .

$V$	= vehicle velocity, $LT^{-1}$
$DP$	= drawbar pull, $MLT^{-2}$
$M$	= mass of vehicle, $M$
$g$	= acceleration due to gravity, $LT^{-2}$
$\mu$	= coefficient of friction, soil to wheel material (dimensionless)
$R$	= radius of wheel, $L$
$\omega$	= angular velocity of the wheel, $T^{-1}$
% slip	= $(R\omega - V)/R\omega$ (dimensionless)
$r$	= soil particle size, $L$
$c$	= cohesion, $ML^{-1}T^{-2}$
$\phi$	= angle of internal friction (dimensionless)

Received May 23, 1963.

\* Assistant Professor, Department of Theoretical and Applied Mechanics.

† Staff Engineer, Defense Operations Division.

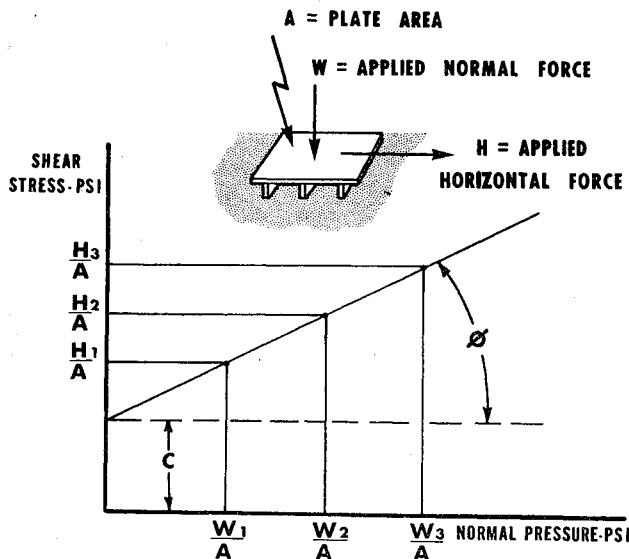


Fig. 1 Definition of cohesion  $c$  and angle of internal friction  $\phi$ .

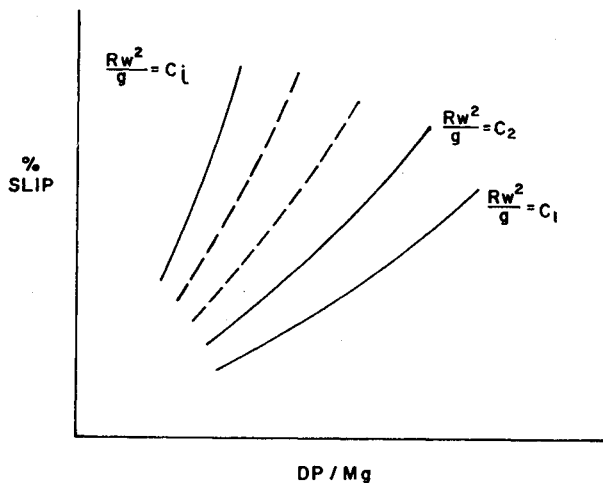


Fig. 2. Family of dimensionless curves.

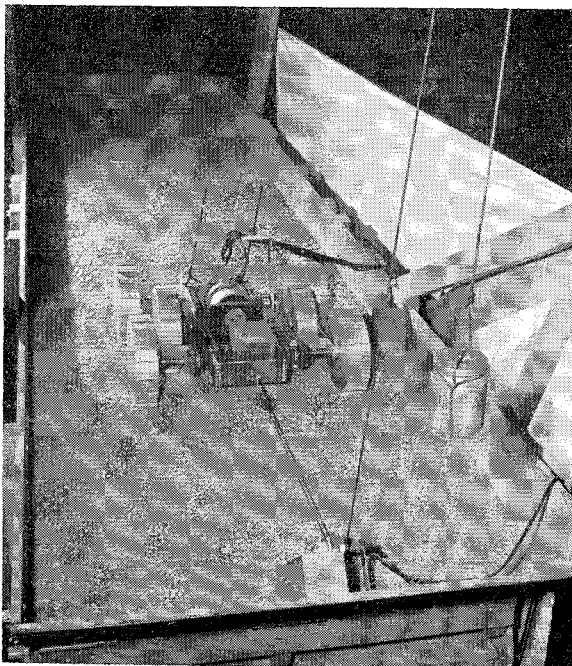


Fig. 3 Test model in soil bin.

- $\rho$  = mass density of the soil,  $ML^{-3}$   
 $E$  = bulk modulus of elasticity,  $ML^{-1} T^{-2}$   
 $\eta$  = viscous property,  $ML^{-1} T^{-1}$

The last six variables are the soil properties as given by Bekker.<sup>1</sup>

The soil values  $c$  and  $\phi$  are defined in Fig. 1.  $c$  is the intercept of the shear stress vs normal pressure curve, at zero normal pressure, whereas  $\phi$  is the slope of the same curve.  $DP$  is a force tangent to the plane of operation. It is equal to the propelling force exerted by the ground on the vehicle minus the resisting forces. The ratio  $DP/Mg$  is the drawbar pull divided by the vehicle weight and is sometimes called the tractive coefficient. It is an approximate measure of a vehicle's ability to tow, bulldoze, accelerate, or climb a hill. The word approximate is used since the vehicle's ability to do these things is modified by such factors as weight transfer and the angle of repose of the soil.

If % slip is chosen as the dependent variable, one may write

$$\% \text{ slip} = F(DP, M, g, \omega, R, r, c, \phi, \rho, \eta, \mu, E)$$

A dimensional analysis<sup>2</sup> yields

$$\% \text{ slip} = f\left(\frac{DP}{Mg}, \frac{R\omega^2}{g}, \frac{M\omega^2}{cR}, \phi, \mu, \frac{\eta^2}{\rho ER^2}, \frac{\rho R^3}{M}, \frac{r}{R}, \frac{c}{E}\right)$$

Since it is very difficult to vary one or more individual properties of the soil while holding the other properties constant, it is inconvenient to use the forementioned analysis to determine the effect of gravity. However, if the soil under consideration is a nonviscous cohesionless soil, e.g., sand or gravel, and if its bulk modulus is neglected,

$$\% \text{ slip} = f\left(\frac{DP}{Mg}, \frac{R\omega^2}{g}, \phi, \mu, \frac{r}{R}, \frac{\rho R^3}{M}\right)$$

It is now possible to hold the variables  $\phi$ ,  $\mu$ ,  $\rho R^3/M$ , and  $r/R$  constant while varying the three remaining variables  $DP/Mg$ ,  $R\omega^2/g$ , and % slip. Thus, curves of the type shown in Fig. 2 can be plotted. The values  $C_1$ ,  $C_2$ , etc. are constants.

Using this method, tests were performed for a six-wheel model (see Fig. 3), operating in  $\frac{1}{4}$ -in. gravel. The data are presented in Fig. 4 and are seen to be scattered about a single line, rather than forming a family of curves as illustrated in Fig. 2. Thus, the ratio of drawbar pull to vehicle weight for a given % slip is practically unaffected by changing  $g$  for the vehicle operating in this soil.

### Conclusions

A dimensional analysis is presented for a rigid vehicle operating in loose soil. This analysis shows that the effect of the gravitational field on the mobility of a vehicle may be determined by changing controlled variables. If the soil is

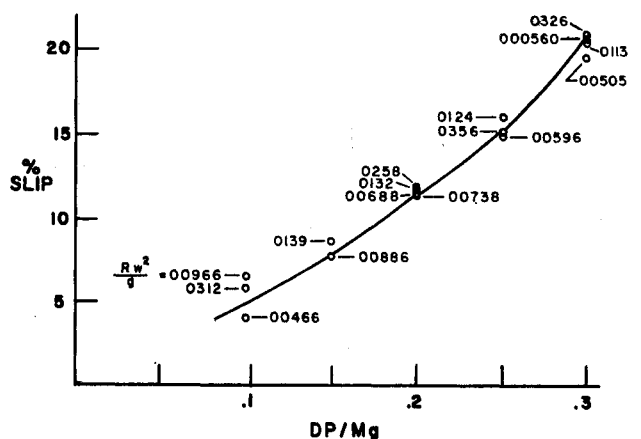


Fig. 4 Test data; drawbar pull/weight for various values of  $R\omega^2/g$ .

characterized by the complete set of Bekker soil values, it is found that several variables must be controlled independently. However, if the soil is a nonviscous, cohesionless soil, such as sand or gravel whose bulk modulus is neglected, it is only necessary to change the vehicle speed to determine the effect of  $g$ . Since many lunar soil investigators have postulated a cohesionless type of soil, the technique of controlling vehicle speed may be all that is necessary. However, consideration is being given to production of artificial soils whose mechanical properties can be varied independently.

In addition, test data are presented for a vehicle model operating in  $\frac{1}{4}$ -in. gravel, which is a nonviscous, cohesionless soil. Test results indicate that the ratio of drawbar pull to vehicle weight is essentially independent of  $g$  for a given % slip. Therefore, it is concluded that, if the vehicle model tested were operating on the lunar surface in a soil with mechanical properties similar to those of the soil used, the vehicle's ability to tow, bulldoze, or accelerate would be reduced by a factor of six, whereas its ability to climb a hill would be unaffected.

### References

- <sup>1</sup> Bekker, M. G., *Theory of Land Locomotion* (The University of Michigan Press, Ann Arbor, 1956), 1st ed., Chap. XI, p. 461.
- <sup>2</sup> Langhaar, H. L., *Dimensional Analysis and Theory of Models* (John Wiley & Sons, New York, 1951), Chap. III, pp. 29 ff.

## Schlieren and Shadowgraph Studies of Hybrid Boundary-Layer Combustion

R. J. MUZZY\*

United Technology Center, Sunnyvale, Calif.

A SERIES of experiments has been performed to check the validity of the hybrid model and analysis of Marxman and Gilbert.<sup>1</sup> The structure of the boundary layer was examined, and the location of the flame zone within the boundary layer was determined.

A small scale wind tunnel was used in the test, and the experiment is shown schematically in Fig. 1. Plexiglas (Polymethyl Methacrylate) slabs 1-in. wide and  $\frac{1}{4}$ -in. high  $\times$  6-in. long were mounted in the test section and ignited in an oxygen stream. Shadowgraph and schlieren studies with a horizontal knife edge then were made of the boundary layer formed over the slab, a system that approximates two-dimensional flow.

A natural parameter that enters into the theoretical development of Marxman and Gilbert<sup>1</sup> is the location of the flame zone within the momentum boundary layer. This parameter was investigated and a 3-msec exposure schlieren photograph appears in Fig. 2. The edge of the thermal boundary layer can be distinguished easily, and if the Lewis and Prandtl numbers are assumed to be near unity, then the edges of the concentration boundary layer, the thermal boundary layer, and the momentum boundary layer are located at the same point.

In analyzing Fig. 2, it is assumed that the gas-density gradients, which cause the schlieren system to respond, are related to temperature variations alone. The density also

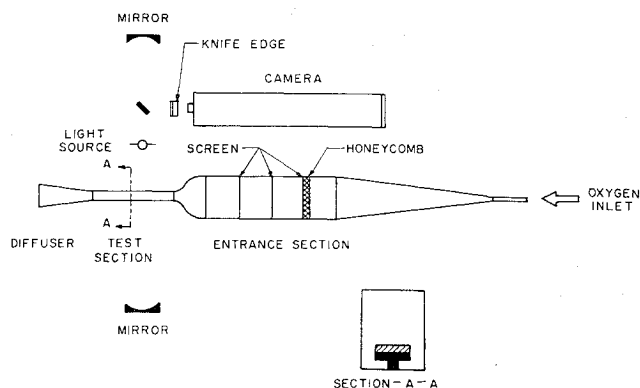


Fig. 1 Experimental apparatus.

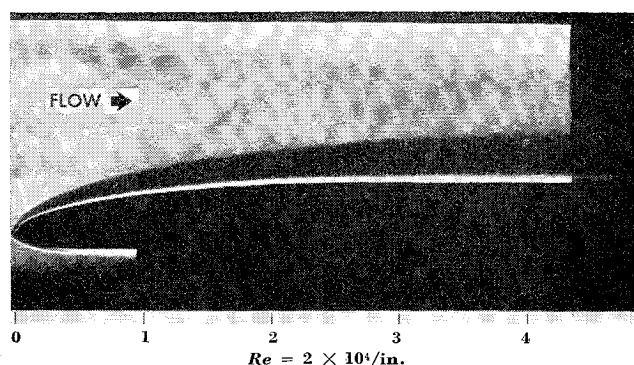


Fig. 2 Schlieren photograph of the combustion boundary layer (exposure time 3 msec).

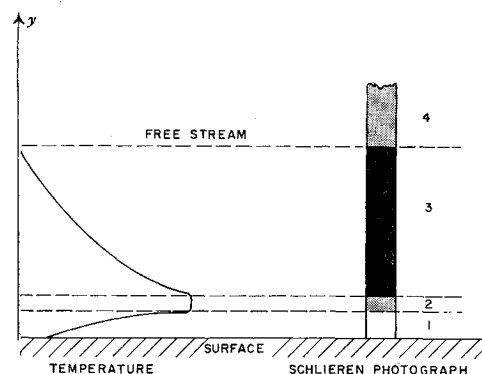


Fig. 3 Interpretation of a typical schlieren photograph.

depends on the local molecular weight of the mixture, but the variations in molecular weight are relatively small.

An interpretation of the schlieren photographs appears in Fig. 3. In order to analyze the photograph, it will be noted that the angular deflection of a ray of light  $\epsilon$  that passes through a schlieren field is proportional to the density according to the relation<sup>2</sup>

$$|\epsilon| \sim (d\rho/dy) \sim (1/T^2)(dT/dy)$$

The gray region 4 in the "freestream" signifies an area of essentially no temperature gradients ( $\epsilon \approx 0$ ). The darker region 3 indicates large negative temperature gradients whereas the lighter region 1 results from strong positive gradients. Dividing these two zones is a second gray region 2, where the temperature goes through a maximum ( $\epsilon \approx 0$ ). The flame lies in this zone.

The uniformity in region 2 gives an indication of the finite thickness of the flame, and, in the present analysis, the flame zone is assumed to lie in the center of this region. Measurements made on this basis indicate that the height of the flame zone above the surface is about  $\frac{1}{10}\delta$  (where  $\delta$  is the measured

Received May 21, 1963. This work was supported by the U. S. Department of the Navy, Bureau of Naval Weapons, Contract N0w-61-1000-c and the Advanced Research Projects Agency. The author is grateful to G. Marxman, C. Wooldridge, M. Gilbert, L. Mahle, and D. La Barbara for their assistance in this investigation.

\* Associate Scientist, Physical Sciences Laboratory. Member AIAA.